HHS Public Access

Author manuscript

*Nat Nanotechnol*. Author manuscript; available in PMC 2014 April 01.

Published in final edited form as:

*Nat Nanotechnol*. 2013 October ; 8(10): 763–771. doi:10.1038/nnano.2013.190.

# Self-assembly of carbon nanotubes and antibodies on tumours for targeted, amplified delivery

**J. Justin Mulvey**[1,4,*], **Carlos H. Villa**[1,4,*], **Michael R. McDevitt**[2,3], **Freddy E. Escorcia**[1,4], **Emily Casey**[1], and **David A. Scheinberg**[1,3,4,5]

[1] Molecular Pharmacology and Chemistry Program, Memorial Sloan-Kettering Cancer Center, New York, New York, 10065

[2]Department of Radiology, Memorial Sloan-Kettering Cancer Center, New York, 10065

[3]Department of Medicine, Memorial Sloan-Kettering Cancer Center, New York, New York, 10065

[4]Weill-Cornell Medical College, New York, New York, 10065

## Abstract

Single-walled carbon nanotubes (SWNTs) can deliver imaging agents or drugs to tumours and offer significant advantages over approaches based on antibodies or other nanomaterials. In particular, the nanotubes can carry a substantial amount of cargo (100 times more than a monoclonal antibody), but can still be rapidly eliminated from circulation by renal filtration, like a small molecule, due to their high aspect ratio. Here we show that SWNTs can target tumours in a two-step approach in which nanotubes modified with morpholino oligonucleotide sequences bind to cancer cells that have been pre-targeted with antibodies modified with oligonucleotide strands complementary to those on the nanotubes. The nanotubes can carry fluorophores or radioisotopes, and were shown to selectively bind to cancer cells *in vitro* and in tumour-bearing xenografted mice. The binding process is also found to lead to antigen capping and internalization of the antibody/nanotube complexes. The nanotube conjugates were labelled with both alpha-particle and gamma-ray emitting isotopes, at high specific activities. Conjugates labelled with alpha-particle generating $^{225}$Ac were found to clear rapidly, thus mitigating radioisotope toxicity, and were shown to be therapeutically effective *in vivo*.

Nanomedicine has begun to produce clinical successes in the first generation of engineered drug nanoparticles[1, 2]. Carbon nanotubes have seen widening application in biomedical research[3], in part because of the potential to append a diverse set of ligands, including small molecules[4], peptides[5, 6], oligonucleotides[7], radioisotopes[8], monoclonal antibodies[9, 10], and other targeting moieties. However, nanoparticle usage is limited by pharmacokinetics, and



[5]Correspondence and requests for materials should be addressed to DAS.

*Contributed equally.

JJM, CV, DAS, and MM conceived and designed the experiments and wrote the paper. CV and JJM conducted all of the experiments. EC assisted with confocal microscopy experiments and FE assisted with solid tumor targeting experiments.

**Additional information**.

Supplementary information accompanies this paper at www.nature.com/naturenanotechnology.

requires modifications to render them suitably water dispersible and biocompatible[11, 12]. Functionalization and dispersion imparts stability in aqueous environments and mitigates toxicity[13]. An important feature of covalently-functionalized SWNTs that allows their use as drug carriers is their extremely rapid clearance via renal glomerular filtration despite large molecular weights[8, 14, 15]. This clearance phenomenon has been termed 'fibrillar pharmacology'[16] and contrasts with the pharmacokinetic profiles of globular proteins.

Typically, in systemic targeting of malignancies, drug delivery vehicles such as mAb or nanoparticles are appended with cytotoxic effectors such as chemotherapeutic small molecules or radioisotopes in a "single-step" process. However, prolonged plasma half-lives of the excess, unbound effector molecules (often exceeding 99.9% of injected species) increase toxicity. In contrast, a short circulation time for a "single step" delivery is problematic as it reduces the time in which a high enough concentration can be maintained in the bloodstream to drive tumour penetration and cell binding.

Two-step targeting ("pre-targeting") separates the slow, non-toxic tumour-targeting process from the necessary rapid clearance of the cytotoxic agent to achieve the desired pharmacokinetic goals[17]. In this approach, a long-circulating tumour selective agent, such as a monoclonal antibody, is first administered and allowed a sufficient circulation time to accumulate at the tumour and clear the bloodstream. This pre-targeting agent is followed by a rapidly cleared second-step agent, armed with cytotoxic or diagnostic effectors, that has a high-affinity for the initial agent. This interaction may involve streptavidin-biotin[18], bispecific antibody-hapten[19], oligonucleotide hybridization[20], or covalent 'click' chemistry[21] interactions. This approach allows for improved ratios of the cytotoxic or imaging agent in the tumour to that in the blood.

Previous successes of pre-targeting have not taken advantage of particulate or nanomaterial second-step vehicles as they typically clear the body slowly and accumulate in organs such as liver and spleen[22, 23]. Small molecules, such as biotin or an oligonucleotide, allow rapid excretion of the second-step reagent[24], but are usually mono-substituted, limiting potency and sensitivity[25, 26]. SWNTs uniquely solve this problem as their structure allows for multiple appended cytotoxic moieties while still clearing rapidly[10, 14].

We chose complementary 18-mer morpholino oligonucleotides to link SWNT vehicles and correspondingly modified monoclonal antibody pre-targeting agents as a high affinity, self-assembling linker strategy. Oligonucleotide base pairing is an attractive approach for binding of nanotubes to antibodies because oligo-modified SWNTs have been described previously[27], and maintain their clearance[7]. If an oligo with a stabilized backbone is employed, such as with the morpholino DNA analogs[20, 28, 29] used in this study, serum degradation[30, 31] is prevented and hybridization occurs *in vivo*.

## SWNT modification, hybridization and radiolabeling

The amine functionalized SWNTs (Figure 1, Structure **1**) used in the current study were prepared from high-purity, arc-discharge or HiPCO produced SWNTs via covalent cycloaddition of azomethine ylides as described previously[9, 14, 32, 33]. This reaction attaches hydrophilic chains to the SWNT sidewalls, terminated with primary amines to serve as the

attachment site for bifunctional radiometal chelates, fluorophores, and the morpholino oligonucleotide complementary to a modified antibody (cMORF). Using chelators appended in such a manner, we produced SWNT-cMORF-DOTA conjugates **(5)** that had been subsequently labeled to high specific activities, up to 25 Ci/g and 20 Ci/g when labeling with $^{111}$In and $^{225}$Ac, respectively. This represents a greater than 100-fold improvement in specific activity of the SWNT-cMORF compared to monoclonal antibodies[10, 34], and demonstrates the potential for signal amplification with highly multivalent SWNT scaffolds.

HPLC of constructs **4, 5**, and **6** in both reverse phase and gel permeation systems demonstrated high purity, and the single peak observed had a spectrum consistent with SWNT appended with bis-aryl hydrazone linkages of $\lambda_{max}$ = 354 nm (Figure 1, c). The Raman spectrum of the amine functionalized SWNTs, **1**, was consistent with highly modified SWNTs, as in previous studies[8, 14]. Four different clinically useful human IgG1 antibody-MORF conjugates were used in this study: anti-CD33-MORF (Lintuzumab) (3.7 MORF per Ab), anti-CD20-MORF (Rituximab) (3.5 MORF per Ab), anti-A33-MORF (huA33) (4.2 MORF per Ab), and anti-CD19-MORF (4.6 MORF per Ab). This approach[35] produced antibody-morpholino conjugates (mAb-MORF) that were >95% pure of non-SWNT molecules, as measured by size-exclusion HPLC.

Hybridization of antibody-MORF with SWNT-cMORF was monitored with HPLC (Figure S1, a–d). The mAb-MORF conjugates alone had an elution time of ~18 minutes, which was consistent with a molecular weight of ~150,000Da based on protein standards. When the mAb-MORF (both anti-CD20-MORF and anti-A33-MORF) was incubated with the complementary SWNT-cMORF, the nanotube elution shifted to a high molecular weight band, and eluted at the void volume (12 minutes) (Figure S1, b). The column's molecular weight cutoff is 600 kDa, suggesting that multiple antibodies had hybridized to each SWNT, forming large, but still soluble, multimeric constructs. We performed a similar experiment with radiolabeled SWNT-cMORF-($^{111}$In)DOTA (Figure 1, **6**), and monitored the elution of the isotope with a HPLC radiodetector, showing an identical pattern of results for SWNT-cMORF mixed with both anti-CD20-MORF and anti-A33-MORF. This confirmed that the assembly of these complexes was independent of the antibody used (Figure S1, c) and the presence of 100% human serum at 37°C (Figure S1, d). The dependence of the observed phenomenon on the MORF/cMORF hybridization, was demonstrated by blocking the nucleotide hybridization sites of the Ab-SWNT complex by addition of excess free cMORF.

Another approach to confirm the hybridization of the SWNT-cMORF conjugate and complementary mAb-MORF was to capture the radiolabeled SWNT-cMORF with protein A beads pre-bound to mAb-MORF (Figure S1, e). When radiolabelled SWNT-cMORF conjugates were incubated with protein A beads alone, only 1% of the nanotubes were captured by the beads. However, when complementary mAb-MORF was added to the SWNT-cMORF shortly before incubation, ~35% of the nanotubes were captured by the beads; capture was completely blocked by addition of excess cMORF to block nanotube hybridization sites on the antibody. Nearly identical binding was obtained in the presence of 100% human serum at 37 °C for 24 hours.

## Self-assembly on pre-targeted cells and in mice

Three different cancer cell lines, Daudi ($CD20^+$ B-cell lymphoma), HL60 ($CD33^+$ myelocytic leukemia), and LS174T ($A33^+$ colon adenocarcinoma) were employed to show that the SWNT-cMORF self-assembles onto tumour cell surfaces pre-treated with specific mAb-MORF conjugates containing the complementary oligonucleotide sequence. These were pre-targeted by anti-CD20 (Rituximab), anti-CD33 (Lintuzumab), and anti-A33 monoclonal antibodies respectively (Figure 1, **4**). The SWNT self-assembled onto all three cell types with high specificity (Figure 2, a–d). The binding was abrogated when blocked with excess cMORF and there was little binding to cells treated with isotype control mAb-MORF. Similar binding was confirmed across a range of conditions, at temperatures of 4, 25, and 37°C as well as in 100% human serum, confirming that MORF/cMORF hybridization onto cells will occur in physiological, laboratory, and storage conditions.

An avidity estimation was performed targeting Daudi cells with anti-CD20-MORF, HL60 cells with anti-CD33-MORF, and LS174T with anti-A33-MORF (Figure 2,) showing an apparent dissociation constant of 0.3 ug/mL, yielding an apparent affinity Kd of ~0.6 nM. This was identical for all three cell types, and thus, was independent of the chosen cancer target or targeting vehicle.

We next assessed self-assembly onto tumours in live mice, initially in the CD20-positive Daudi lymphoma model. SCID mice were injected with Daudi-GFP[9] cells i.p, followed 24 hours later with injection of either lymphoma-specific anti-CD20-MORF or anti-CD33-MORF isotype control. The mice were treated 24 hours later with fluorescently labeled SWNT-cMORF 24 hours later, and after 6 hours, were sacrificed, and the lymphoma cells were analyzed by flow cytometry. We observed a 20-fold increase in the median fluorescence intensity of the gated Daudi cells in the FL4 channel (Figure 4, a–b) from the anti-CD20 mAb-MORF treated animal, confirming specific assembly on the harvested cells. The isotype control antibody (anti-CD33-MORF) treated animals did not demonstrate binding or self-assembly.

A subcutaneous, xenografted, solid tumour (LS174T colon adenocarcinoma model,) in which tumour penetration of each of the components is more difficult, was targeted with i.v. anti-A33 antibody. After 24 hours, SWNT-cMORF-($^{111}$In)DOTA second step was administered in the same fashion. The accumulation of SWNT-cMORF-($^{111}$In)DOTA in blood and tumour were quantified at 4 and 24 hours (Figure 4, c). The SWNT-cMORF-($^{111}$In)DOTA rapidly cleared the blood with levels of 1.4 %ID/g and 0.26 % ID/g at 4 and 24 hours, respectively[14]. At 24 hours, SWNT-cMORF was better retained in the tumours of specifically targeted animals than at 4 hours, and there was a modest, but significant increase in the tumour to blood ratio for the specifically targeted tumours versus the isotype control (Figure 4, c). Unlike tumour in Figure 4c, no other measured tissues showed significant enhancement of specifically treated cells versus the isotype (Figure S3). As with other soluble SWNT constructs[8], we observed off-target accumulation of the unbound molecule in the kidneys. A time-based biodistribution of the injected SWNT second step construct in selected organs is provided (Figure S4) as well as a more complete clearance analysis at 24 hours post-injection (Figure S5).

## Self-assembly on cells leads to capping and internalization

We also wanted to determine the fate of the self-assembled SWNT-cMORF/mAb-MORF complexes on the cell surface. Confocal microscopy studies were used to track anti-A33 antibodies and anti-A33/SWNT complexes after assembly on the LS174T cells and incubated at 37°C in culture medium for up to 24 hours. When cells were treated with the anti-A33 antibody alone (green), the antibody was stable on the cell surface for up to 24 hours (Figure 3, column a). A33 was chosen for this demonstration due to its slow internalization and lysosomal degradation with a turnover of 6 weeks at 37°C[36, 37], similar to CD20[38], used in our therapy studies. The anti-A33-MORF antibody conjugate alone was stable on the cell surface and remained evenly distributed (Figure 3, column b). However, when SWNT-cMORF (pink) was added to anti-A33-MORF pre-targeted cells, followed by up to 4 hours of incubation at 37°C, we observed a dramatic change in the distribution of antibody in the target cells (Figure 3, column c) including clustering of the self-assembled mAb-MORF/SWNT-cMORF complexes on the cell membrane, leading to punctate staining suggestive of antigen capping (Figure 3, schematic f (c1)). Relevant controls did not result in any change in staining pattern.

This clustering phenomenon continued to increase through the 4 hours assayed, suggesting an endocytic uptake of the anti-A33-MORF/SWNT-cMORF complexes upon self-assembly into multimeric surface structures, separate from internalization of individual A33 molecules. Therefore, as SWNT-cMORF constructs can bind multiple antibodies on the cell surface, this cross-linking apparently leads to promotion of rapid intracellular delivery of the complexes in line with observations of cross-linking upon prolonged mixing of SWNT-cMORF and Ab-MORF (Figure S1). To test this hypothesis, we treated anti-A33-MORF targeted cells with free cMORF oligonucleotides, which should not bind multiple antibodies. When cells pretreated with anti-A33-MORF were subsequently treated with fluorescently labeled cMORF alone, the staining profile of the cMORF was completely co-localized with the antibody and the pattern of surface binding was unchanged from antibody alone (Figure 3, d and f (d1) - compare with a,b). This result suggests that the capping and internalization phenomenon depended on the multivalency of the second step. While not imperative to this study, this finding may predict endocytotic delivery through cross-linking for some surface markers that are known to slowly internalize, and implicates SWNTs as an effective tool for such plaque formation.

## SWNT-cMORF-DOTA as a vehicle for $^{225}$Ac mitigates toxicity

To demonstrate that the SWNT-cMORF constructs would be effective in a therapeutic model of human lymphoma using a xenografted SCID mouse model, we conducted a dose-escalation toxicity study and biodistribution in vivo. The rapid clearance of the secondary agent should offer an improved therapeutic index due to reduced circulation time of the cytotoxic effector. In accordance with our previous clearance studies[7, 8, 14], biodistribution experiments performed with SWNT-cMORF-($^{111}$In) showed that the majority of the total injected dose (~77% ID) was excreted (largely in urine) by 24 hours, and no organ other than the kidney had more than 0.2% of the injected dose per gram after one hour (Figure S4, S5).

This rapid clearance of radiolabeled SWNT markedly reduced toxicity in mice when compared to similarly radiolabeled “single step” monoclonal antibodies, free $^{225}$Ac, or antibodies labeled with the MORF directly. For monoclonal antibodies directly labeled with $^{225}$Ac, the maximum tolerated dose in mice is 450nCi in a single injection, while for $^{225}$Ac alone (Figure 5a) this dose was rapidly lethal[34, 39–41].

Although we observed dose-dependent body weight loss and organ weight loss in mice receiving the radiolabeled SWNT-cMORF-($^{225}$Ac)DOTA (Figure 5a, S6), all mice administered with SWNT-cMORF-($^{225}$Ac)DOTA below 2250 nCi survived through the 140 day experiment. One of five mice and two of five mice died in the 2250 nci and 2700 nCi groups respectively. Mice at dose levels of 1350 to 2700 nCi showed limited dose-dependent toxicity including reduced bone marrow and splenic cellularity and smaller glomeruli at 140 days (Figure S6).

The pre-annealed “single-step” toxicity study conducted for comparison demonstrated that all dosing groups (450–1800nCi) reached a dose-dependent, terminal morbidity starting at six days post injection, presumably from the annealed structure’s inability to clear the kidneys (Figure 5b, S7). The maximum tolerated dose of the pre-annealed material (<450nCi) was reached at a dose at least six-fold lower than when using the nanotube carrier (>2700nCi) and median survival was at least 10 fold shorter (<2 weeks vs >20 weeks.) The rapid lethality of the one step approach prohibited a direct comparison of the two strategies in therapy models.

## Therapy with SWNT-cMORF-($^{225}$Ac)DOTA

Mice were implanted with Daudi lymphoma cells in the peritoneal cavity followed by multistep therapy one week later, after tumour confirmation. The study included 10 groups of 5 mice each, consisting of 3 treatment groups and 7 control groups (Methods Table 1). Tumour imaging studies demonstrated effective dose-dependent therapy in all 3 treatment groups (Figure 6, S8). There was complete elimination of tumour burden in treatment groups 8 and 9 (666 nCi SWNT-cMORF-($^{225}$Ac)DOTA and 999 nCi SWNT-cMORF-($^{225}$Ac)DOTA. Mice in the saline control, and cold SWNT control showed rapid progression of tumour burden. Mice treated with anti-CD20-MORF alone showed a brief reduction in tumour load that was attributed to a transient response to the unlabeled anti-CD20 antibody, which is known to be a potent therapeutic alone (Rituximab). Mice treated with the isotype control anti-CD33-MORF followed by SWNT-cMORF-($^{225}$Ac)DOTA at several dose levels showed transient responses, attributable to non-specific irradiation from Ac-225. Finally, to demonstrate that the therapeutic effect was due to self-assembly and not simply additive effects of each component of the therapy, we included a dual control of anti-CD20-MORF followed by SWNT-cMORF-($^{225}$Ac)DOTA that had been mixed with excess free MORF to block hybridization. In this group, four of five mice had marked tumour progression, while one mouse had a therapeutic response attributed to the additive effects of anti-CD20-MORF and non-specific radiation.

The SWNT construct has the advantage over a small molecule of vastly amplified delivery of cytotoxic moieties. This was shown by direct conjugation of cMORF through its terminal

amine to DOTA chelators (cMORF-DOTA), similar to work pioneered by Hnatowich et al.[31]. The SWNT's carrying capacity due to sheer size (~ 430,000 Daltons – calculated via equation in Figure S11) allows the maximum delivery of ~115 $^{225}$Ac cytotoxic moieties per bound second-step molecule compared to a maximum of 1 can be delivered through a cMORF-DOTA small-molecule construct. In addition, cMORF-($^{111}$In) DOTA delivered ~1% of the radioactivity of that of SWNT-cMORF-DOTA second-step (Figure S9) with less non-specific accumulation.

Antibody-drug conjugate and radioimmunotherapy strategies to treat cancer have been limited by poor therapeutic indexes. The high aspect ratio of carbon nanotubes offers unique properties that makes them desirable carriers in cancer drug delivery and distinguish them from antibodies or other nano-particulate carriers. Foremost among these features are the pharmacological ability of SWNT carriers to be rapidly and efficiently eliminated from circulation by renal filtration, and to carry orders of magnitude more ligands than conventional vehicles like mAbs[14].

Having shown the feasibility of the model through toxicity studies, we next demonstrated that carbon nanotubes can target tumours in a multistep approach. We synthesized covalently modified SWNT bearing multiple copies of morpholino oligonucleotides, fluorophores, and radioisotopes. The SWNT-cMORF conjugates were capable of specific self-assembly onto antibody targeted cancer cells *in-vitro* and in mice with potent therapeutic effects in xenograft tumours. In addition, the ability to trigger internalization of a surface antigen through SWNT-cMORF self-assembly is promising, and may enhance therapeutic efficacy of agents appended to the SWNT for some targets. The second step in such a self-assembly approach could also be used as a trigger for internalization of the initial targeting agent, further diversifying the utility of this approach and improving the therapeutic index.

These SWNT-cMORF -$^{225}$Ac, constructs, demonstrated rapid clearance with resultant five to ten-fold reduction of toxicity when compared to a single-step (pre-annealed) approach. While the use of a small molecule as the second step vehicle was found to be feasible, it lacked amplification by two orders of magnitude. The further application of SWNT-cMORF conjugates as imaging and therapeutic agents, particularly in the context of the pharmacologic challenges of delivery to solid tumours, requires careful optimization to improve the tumour to normal tissue ratios with regard to the timing, dose levels, and point of injection in a two-step strategy[42]. Engineering the SWNT properties, such as surface charge, is likely to further minimize non-specific accumulation by the reticuloendothelial system and reabsorption by renal proximal tubules[7, 8, 14,43]. These findings highlight the importance of engineering a particle targeting strategy to take full advantage of the nanomaterial's pharmacokinetic and pharmacodynamic behaviors. Such strategies are able to exploit the properties that arise from nanoscale physical features, and move towards a feasible nanomedicine.

## Methods

### Modification of SWNT and antibodies

High purity (>90% SWNT) single walled carbon nanotubes were obtained from NanoLab Inc (Waltham, MA) and purified[33] (Supplemental methods and Figure S10). Morpholino oligonucleotides were custom synthesized (Gene Tools Inc.) and contained primary amines on the 3' end. The primary amine was capped with either an aldehyde or hydrazine moiety for conjugation to the antibodies or nanotubes, respectively. Monoclonal antibodies HuM195/Lintuzumab/anti-CD33; (Sloan-Kettering), Rituximab/anti-CD20 (Genentech), and huA33/anti-A33 (Ludwig Institute) were conjugated to the oligonucleotide and purified (See Supplementary methods.)

### In Depth Characterization of Constructs

Constructs averaged 350 nm in length by DLS and TEM with diameter of approximately 1.2nm giving 12 carbon atoms per 2.5 angstroms. They were characterized by Raman spectroscopy, a spectrally quantifiable bis-aryl hydrazone linkage between the two entities[6, 35], and for amine content by a quantitative ninhydrin assay[44] The average unmodified and modified nanotube molecular weight (434,968.20 g/mol, ~1.22E6 g/mol) derivation is provided (Figure S11). Custom synthesized morpholinos[45], bearing 3' primary amines were reacted with succinimidyl hydrazine nicotinamide and purified to yield the cMORF-HyNic product. The cMORF-HyNic was coupled with the aldehyde functionalized SWNT to yield the SWNT-cMORF conjugate (Figure 1a, **3**). The remaining amines in compound **3** were then either modified with the radiometal chelating moiety, DOTA, for subsequent labeling with radiometals (Figure 1a, **5**), or reacted with the activated ester of Alexa Fluor 647 to introduce a fluorescent label for microscopy and cytometric assays (Figure 1a, **4**) to yield 1 DOTA or Alexa Fluor per 316 carbon atoms or approximately 115 adducts per median-lengthed tube The DOTA chelator was labelled $^{111}$In was used for biodistribution and binding studies or $^{225}$Ac, an alpha-particle emitting cytotoxic isotope for toxicity and therapeutic models.

### Binding studies in mice

Each mouse was injected with 20 million cells. After 6 hours, the mice were treated with 3 ug of morpholino conjugates of either Daudi specific anti-CD20 Rituximab (anti-CD20-MORF) or isotype control anti-CD33 HuM195 (anti-CD33-MORF). 16 hours later, mice were injected i.p. with 2 ug of SWNT-cMORF-AF647. The SWNT-cMORF-AF647 was allowed to circulate and bind for 4 hours, after which mice were sacrificed and the lymphoma cells collected by lavage of the i.p. cavity with 0°C PBS. For solid tumour studies, 5–7 week old female NCI nu/nu mice were xenografted with 5 million LS174T cells subcutaneously into the right flank. Once tumours reached ~150 mm$^3$, at about 7 days, mice were treated with i.p. injection of 20 ug of either tumour specific anti-A33-MORF or isotype control anti-CD33-MORF antibodies diluted in normal saline. 72 hours after treatment with the antibodies, the mice were injected with 12 ug of SWNT-cMORF-($^{111}$In)DOTA intravenously via the retro orbital sinus. At various time points mice were sacrificed, their organs harvested and weighed; the radioactivity was counted on a Cobra II gamma counter (Packard).

### Toxicology study in mice: SWNT-cMORF-DOTA

SWNT-cMORF-DOTA were labeled with $^{225}$Ac at a 98.4% radio-chemical purity. 45 BALB/c mice (NCI Labs,) age 5–7 weeks. Mice were randomly divided into 9 groups of 5 mice and received a single injection as described (Supplementary methods Table S1). Each group was visually assessed and weighed regularly over 140 days. Histological evaluation was performed by a MSKCC veterinary pathologist blinded to the treatment groups.

### Toxicology study in mice: Pre-annealed Ab-MORF--SWNT-cMORF-DOTA($^{225}$Ac)

Mice were randomly divided into 7 groups of 5 mice and received a single injection as described (Supplemental methods Table S2): Mice were followed until death or weight stabilization had occurred.

### Therapy study in mice

SWNT-cMORF-DOTA were labeled with $^{225}$Ac at a 96% radiochemical purity. CB17SC-F SCID mice (Taconic Labs,) age 5–7 weeks, were injected I.P. with 20 million firefly-luciferase expressing Daudi lymphoma cells. After one week, mice were imaged to confirm establishment of tumour, then randomly assigned into 10 treatment groups of 5 mice each (Table 1) that received two sequential injections at 0 and 24 hours. Mice were imaged and photons quantitated for tumour burden on day 3, 6, 9 and 15 after the injection of the second step.

For additional Methods, please see supplementary information.

## Supplementary Material

Refer to Web version on PubMed Central for supplementary material.

## Acknowledgements

We would like to acknowledge support from NIH P01 CA33049 (DAS), NIH R01 CA55349 (DAS), R21 CA128406 (MRM), Office of Science (BER), U. S. Department of Energy (Award DE-SC0002456) (MRM), NIH Medical Scientist Training Program [MSTP] Grant GM07739 (JJM, CHV, FEE), the MSKCC Molecular Cytology Core Facility, the MSKCC Experimental Therapeutics Center, the MSKCC Brain Tumour Center, The Tudor and Glades Funds, and Donald Hnatowich for helpful discussions. We thank W. Maguire, S. Alidori and E. Feinberg for assistance and Actinium Pharmaceuticals for $^{225}$Ac acquisition. We thank M. Bergkvist for TEM and Raman spectroscopy.

## References

1. Scheinberg DA, Villa CH, Escorcia FE, McDevitt MR. Conscripts of the infinite armada: systemic cancer therapy using nanomaterials. Nat. Rev. Clin. Oncol. 2010; 7:266–276. [PubMed: 20351700]
2. Davis ME, Chen ZG, Shin DM. Nanoparticle therapeutics: an emerging treatment modality for cancer. Nat. Rev. Drug Discov. 2008; 7:771–782. [PubMed: 18758474]
3. Kostarelos K, Bianco A, Prato M. Promises, facts and challenges for carbon nanotubes in imaging and therapeutics. Nature Nanotech. 2009; 4:627–633.
4. Liu Z, et al. Drug delivery with carbon nanotubes for in vivo cancer treatment. Cancer research. 2008; 68:6652–6660. [PubMed: 18701489]
5. Liu Z, et al. In vivo biodistribution and highly efficient tumour targeting of carbon nanotubes in mice. Nature Nanotech. 2007; 2:47–52.

6. Villa CH, et al. Single-Walled Carbon nanotubes deliver peptide antigen into dendritic cells and enhance IgG responses to tumour-associated antigens. ACS Nano. 2011; 5:5300–5311. [PubMed: 21682329]
7. Villa CH, et al. Synthesis and biodistribution of oligonucleotide-functionalized, tumour-targetable carbon nanotubes. Nano Lett. 2008; 8:4221–4228. [PubMed: 19367842]
8. McDevitt MR, et al. PET imaging of soluble yttrium-86-labeled carbon nanotubes in mice. PLoS ONE. 2007; 2:e907. [PubMed: 17878942]
9. McDevitt MR, et al. Tumour targeting with antibody-functionalized, radiolabeled carbon nanotubes. J. Nucl. Med. 2007; 48:1180–1189. [PubMed: 17607040]
10. Ruggiero A, et al. Imaging and treating tumour vasculature with targeted radiolabeled carbon nanotubes. Int. J. Nanomed. 2010; 5:783–802.
11. Singh R, et al. Tissue biodistribution and blood clearance rates of intravenously administered carbon nanotube radiotracers. Proc. Natl Acad. Sci. USA. 2006; 103:3357–3362. [PubMed: 16492781]
12. Liu Z, et al. Circulation and long-term fate of functionalized, biocompatible single-walled carbon nanotubes in mice probed by Raman spectroscopy. Proc. Natl Acad. Sci. USA. 2008; 105:1410–1415. [PubMed: 18230737]
13. Mutlu GKM, et al. Biocompatible Nanoscale Dispersion of Single-Walled Carbon Nanotubes Minimizes in vivo Pulmonary Toxicity. Nano Lett. 2010; 10:1664–1670. [PubMed: 20377197]
14. Ruggiero A, et al. Paradoxical glomerular filtration of carbon nanotubes. Proc. Natl Acad. Sci. USA. 2010; 107:12369–12374. [PubMed: 20566862]
15. Lacerda L, et al. Carbon-nanotube shape and individualization critical for renal excretion. Small. 2008; 4:1130–1132. [PubMed: 18666166]
16. Kostarelos K. Carbon nanotubes: Fibrillar pharmacology. Nature Mater. 2010; 9:793–795. [PubMed: 20864939]
17. Goldenberg D, Sharkey R, Paganelli G, Barbet J. Antibody Pretargeting Advances Cancer Radioimmunodetection and Radioimmunotherapy. J. Clin. Oncol. 2006; 10:823–834. [PubMed: 16380412]
18. Green DJ, et al. Pretargeted radioimmunotherapy for B-cell lymphomas. Clin. Cancer Res. 2007; 13:5598s–5603s. [PubMed: 17875795]
19. Sharkey RM, et al. Improved therapy of non-Hodgkin's lymphoma xenografts using radionuclides pretargeted with a new anti-CD20 bispecific antibody. Leukemia. 2005; 19:1064–1069. [PubMed: 15815716]
20. Liu G, et al. Successful radiotherapy of tumour in pretargeted mice by 188Re-radiolabeled phosphorodiamidate morpholino oligomer, a synthetic DNA analogue. Clin. Cancer. Res. 2006; 12:4958–4964. [PubMed: 16914585]
21. Rossin R, et al. In vivo chemistry for pretargeted tumour imaging in live mice. Angew. Chem. Int. Ed. 2010; 49:3375–3378.
22. Park J-H, et al. Cooperative nanomaterial system to sensitize, target, and treat tumours. Proc. Natl Acad. Sci. USA. 2010; 107:981–986. [PubMed: 20080556]
23. Perrault SD, Chan WCW. In vivo assembly of nanoparticle components to improve targeted cancer imaging. Proc. Natl Acad. Sci. USA. 2010; 107:11194–11199. [PubMed: 20534561]
24. Liu G, et al. Adding a clearing agent to pretargeting does not lower the tumour accumulation of the effector as predicted. Cancer Biother. Radio. 2010; 25:757–762.
25. Alvarez-Diez TM, Polihronis J, Reilly RM. Pretargeted tumour imaging with streptavidin immunoconjugates of monoclonal antibody CC49 and 111In-DTPA-biocytin. Nucl. Med. and Biol. 1996; 23:459–466. [PubMed: 8832700]
26. He J, et al. Affinity Enhancement Pretargeting: Synthesis and Testing of a (99m)Tc-Labeled Bivalent MORF. Mol. Pharm. 2010; 2:1118–1124. [PubMed: 20507096]
27. Staii C, Johnson AT, Chen M, Gelperin A. DNA-decorated carbon nanotubes for chemical sensing. Nano Lett. 2005; 5:1774–1778. [PubMed: 16159222]
28. Liu G, et al. Tumour pretargeting in mice using (99m)Tc-labeled morpholino, a DNA analog. J. Nucl. Med. 2002; 43:384–391. [PubMed: 11884499]

29. Moulton HM, et al. Peptide-Morpholino conjugate: A promising therapeutic for Duchenne Muscular Dystrophy. Ann. N.Y. Acad. Sci. 2009; 1175:55–60. [PubMed: 19796077]
30. Park SY, et al. DNA-programmable nanoparticle crystallization. Nature. 2008; 451:553–556. [PubMed: 18235497]
31. Hnatowic DJ, Nakamura K. The influence of chemical structure of DNA and other oligomer radiopharmaceuticals on tumour delivery. Curr. Opin. Mol. Ther. 2006; 8:136–143. [PubMed: 16610766]
32. Georgakilas V, et al. Organic functionalization of carbon nanotubes. J.A.C.S. 2002; 124:760–761. [PubMed: 11817945]
33. Georgakilas V, et al. Amino acid functionalisation of water soluble carbon nanotubes. Che.m Commun. (Camb.). 2002:3050–3051.
34. McDevitt MR, et al. Tumour therapy with targeted atomic nanogenerators. Science. 2001; 294:1537–1540. [PubMed: 11711678]
35. He J, et al. An improved method for covalently conjugating morpholino oligomers to antitumour antibodies. Bioconjug. Chem. 2007; 18:983–988. [PubMed: 17385902]
36. Ackerman ME, et al. A33 antigen displays persistent surface expression. Cancer Immunol. Immunother. 2008; 57:1017–1027. [PubMed: 18236042]
37. Welt S, et al. Phase I study of anticolon cancer humanized antibody A33. Clin. Cancer Res. 2003; 9:1338–1346. [PubMed: 12684402]
38. Golay J, et al. Biologic response of B lymphoma cells to anti-CD20 monoclonal antibody rituximab in vitro: CD55 and CD59 regulate complement-mediated cell lysis. Blood. 2000; 95:3900–3908. [PubMed: 10845926]
39. Miederer M, Scheinberg D, McDevitt M. Realizing the potential of the Actinium-225 radionuclide generator in targeted alpha particle therapy applications. Adv. Drug Deliv. Rev. 2008; 60:1371–1382. [PubMed: 18514364]
40. Song H, et al. Radioimmunotherapy of breast cancer metastases with alpha-particle emitter 225Ac: comparing efficacy with 213Bi and 90Y. Cancer Res. 2009; 69:8941–8948. [PubMed: 19920193]
41. Miederer M, et al. Pharmacokinetics, dosimetry, and toxicity of the targetable atomic generator, 225Ac-HuM195, in nonhuman primates. J. Nucl. Med. 2004; 45:129–137. [PubMed: 14734685]
42. Liu G, Hnatowich DJ. A semiempirical model of tumour pretargeting. Bioconjug. Chem. 2008; 19:2095–2104. [PubMed: 18839978]
43. Vegt E, et al. Renal toxicity of radiolabeled peptides and antibody fragments: mechanisms, impact on radionuclide therapy, and strategies for prevention. J. Nucl. Med. 2010; 51:1049–1058. [PubMed: 20554737]
44. Kaiser E, Colescott RL, Bossinger CD, Cook PI. Color test for detection of free terminal amino groups in the solid-phase synthesis of peptides. Anal. Biochem. 1970; 34:595–598. [PubMed: 5443684]
45. Liu G, et al. Predicting the biodistribution of radiolabeled cMORF effector in MORF-pretargeted mice. Eur. J. Nucl. Med. Mol. I. 2007; 34:237–246.

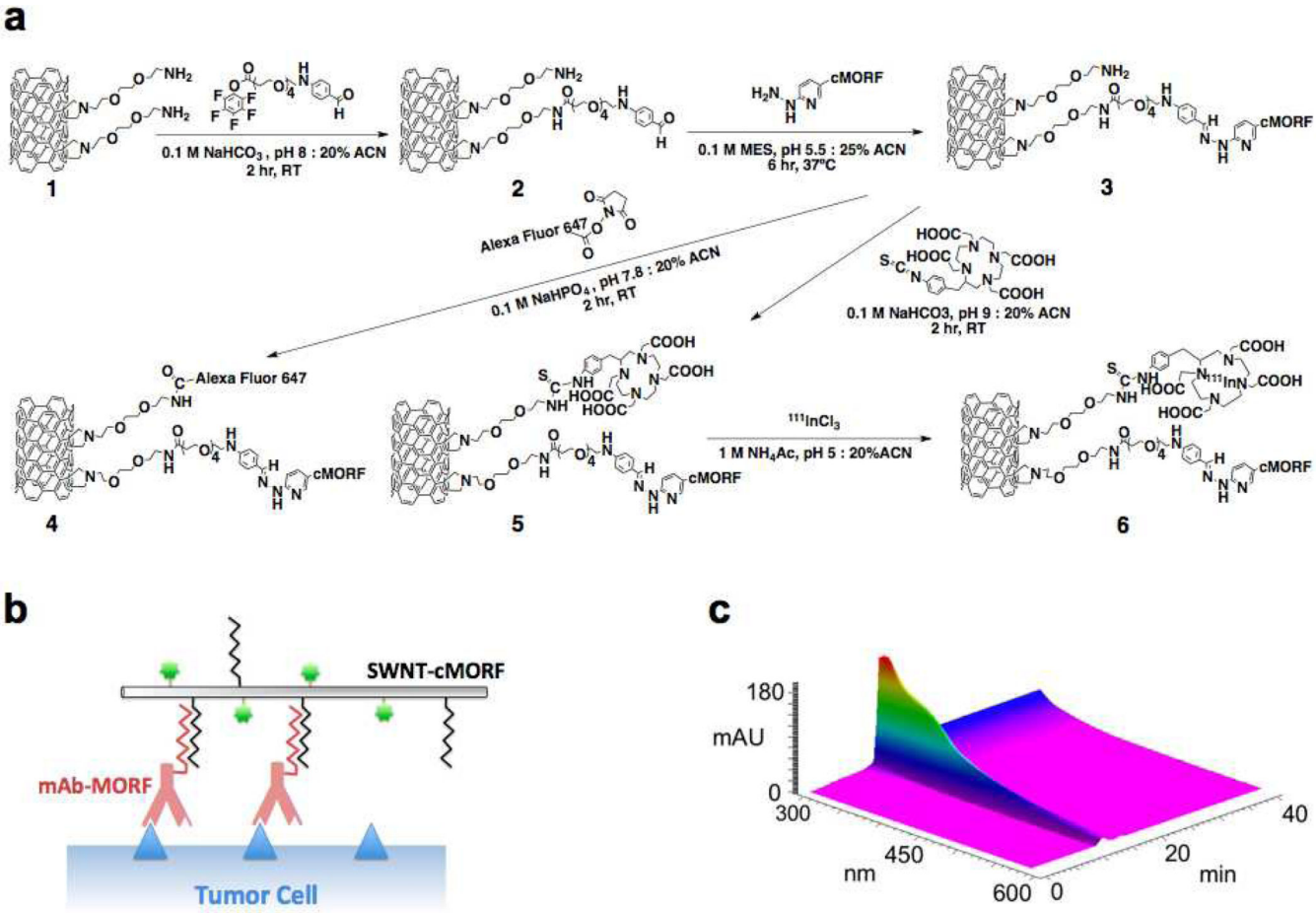


**Figure 1. Design and HPLC characterization of self-assembling SWNT-cMORF constructs**

(a) Synthetic scheme for chemical functionalization of SWNT-$NH_2$ to produce radio- and fluorescent labeled SWNT-cMORF conjugates (b) Diagrammatic representation (not to scale) of SWNT-cMORF self-assembly onto mAb-MORF targeted tumour cells. Blue triangle is tumour antigen; green dot is appended cytotoxic or diagnostic moiety. (c) 3D gel permeation HPLC chromatograph of compound 3 (SWNT-cMORF-$NH_2$) tracing the spectrum of eluted material across time. Only a single peak is evident and the spectrum is consistent with SWNT modified with bis-aryl hydrazone groups (shoulder at $\lambda$ = ~354 nm and decreasing absorption through 600nm – an identifying quality of nanotubes)

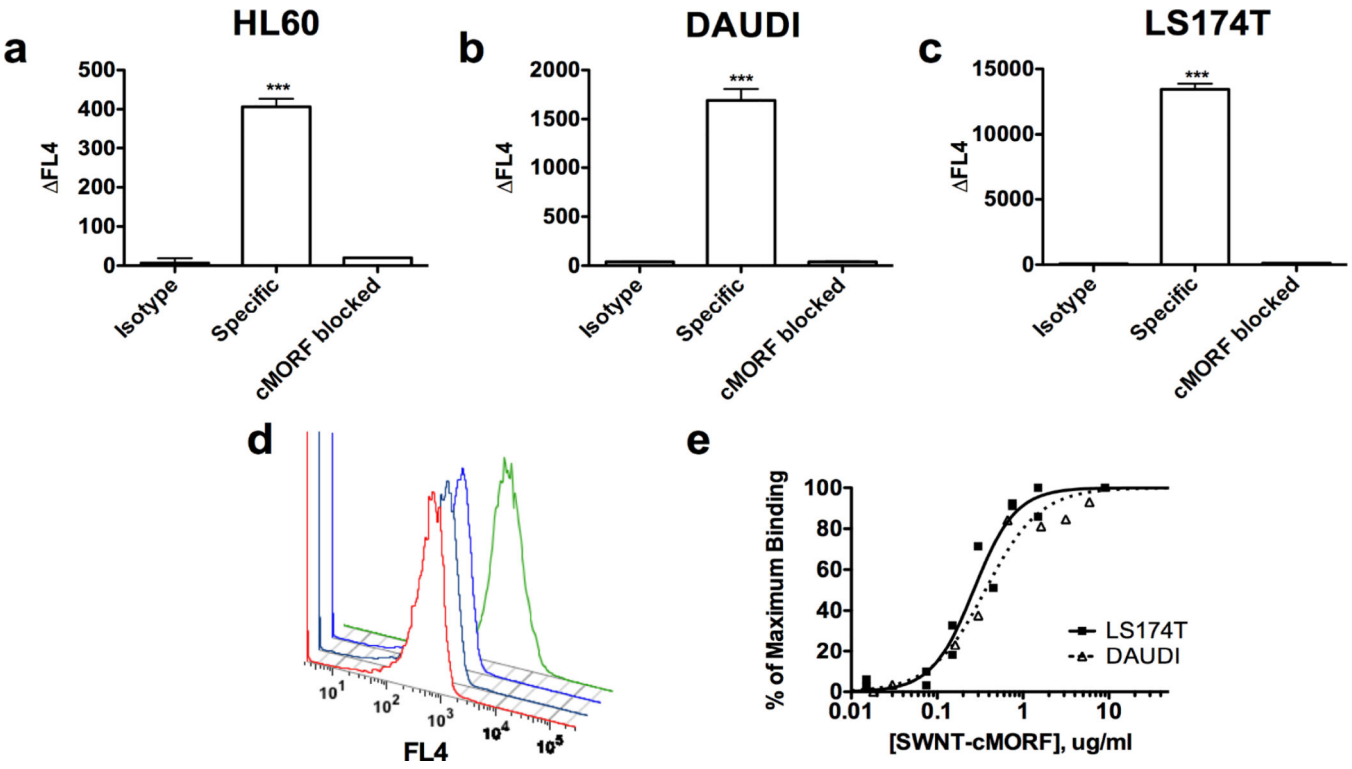


**Figure 2. Self-assembly of SWNT-cMORF onto tumour cells pretargeted with mAb-MORF is highly specific and high affinity**

**a**) Quantitation of flow cytometric assay of binding of SWNT-cMORF-AF647 onto HL60 cells. Pretreatment was with HL60 specific anti-CD33-MORF, isotype control anti-CD20-MORF, or specific anti-CD33-MORF + blocking with excess free cMORF. Data is presented as the change in median fluorescence. **(b)** Quantitation of flow cytometric assay of binding of SWNT-cMORF-AF647 onto DAUDI cells. Pretreatment was with DAUDI specific anti-CD20-MORF, isotype control anti-CD33-MORF, or specific anti-CD20-MORF + blocking with excess free cMORF. **(c)** Quantitation of flow cytometric assay of binding of SWNT-cMORF-AF647 onto LS174T cells. Pretreatment was with LS174T specific anti-A33-MORF, isotype control anti-CD33-MORF, or specific anti-A33-MORF + blocking with excess free cMORF. **(d)** Representative flow cytometric histogram of cell binding assay with SWNT-cMORF-AF647 on untreated (red), isotype control pretargeted (black), specific pretargeted + cMORF block (blue), or specific pretargeted (green) LS174T cells. **(e)** Binding curve for SWNT-cMORF-AF647 onto anti-CD20 pretargeted Daudi cells (squares) and anti-A33 pretargeted LS174T cells (triangles). Curves were fit using GraphPad Prism using an algorithm for one-site specific binding with variable Hill slope ($R^2$ = 0.95, 0.97).

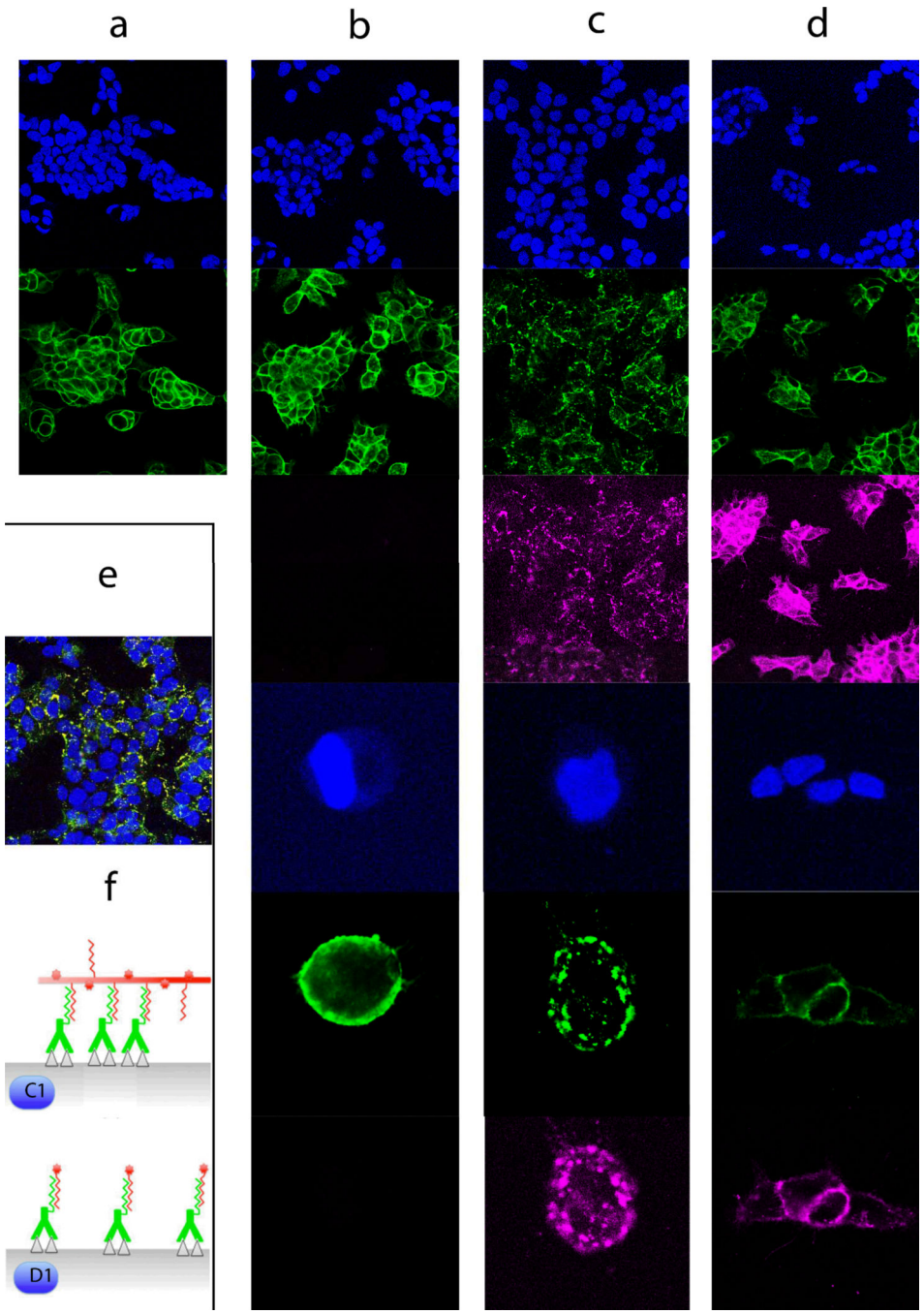


**Figure 3. SWNT-cMORF conjugates are able to induce antigen capping and internalization when self-assembled onto cells targeted with mAb-MORF (images organized in columns)**

**(a)** Anti-A33 (green, row 2) remained stably bound to LS174T cells (blue, DAPI nuclear stain, row 1) at 37°C for up to 24 hours (4 hours is shown) and were evenly distributed about the cell membrane. **(b)** Anti-A33-MORF conjugates (green, row 2,5) exhibited similar surface stability when bound to LS174T cells (blue, rows 1,3). High power images are provided (rows 4,5,6), as well 647nm views showing the absence signal (rows 3,6) **(c)** Cells pretreated with A33-MORF (green, rows 2,5) followed by SWNT-cMORF-AF647 (pink,

rows 3,6), allowing for self-assembly at 37°C for up to 4 hours, demonstrated a significant change in the distribution of the bound antibody with a change to scattered punctate staining. A similar pattern was observed for 30 min and 1 hr incubations. High power images are provided (rows 4,5,6). **(d)** Cells treated with anti-A33-MORF (green, rows 2,5) followed by cMORF-AF647 (pink, rows 3,6) alone did not demonstrate change in distribution of A33 about the cell membrane. High power images are provided (rows 4,5,6). Anti-A33-MORF was evenly distributed about the plasma membrane, and cMORF-AF647 co-localized with the targeted mAb-MORF. **(e)** A composite staining of conditions in (c) with pink and green forming a yellow overlay (enlargement provided in Figure S2). **(f)** Schematic model of self-assembly process and cross-linking shown (not to scale) illustrating conditions of columns (c), above and (d).

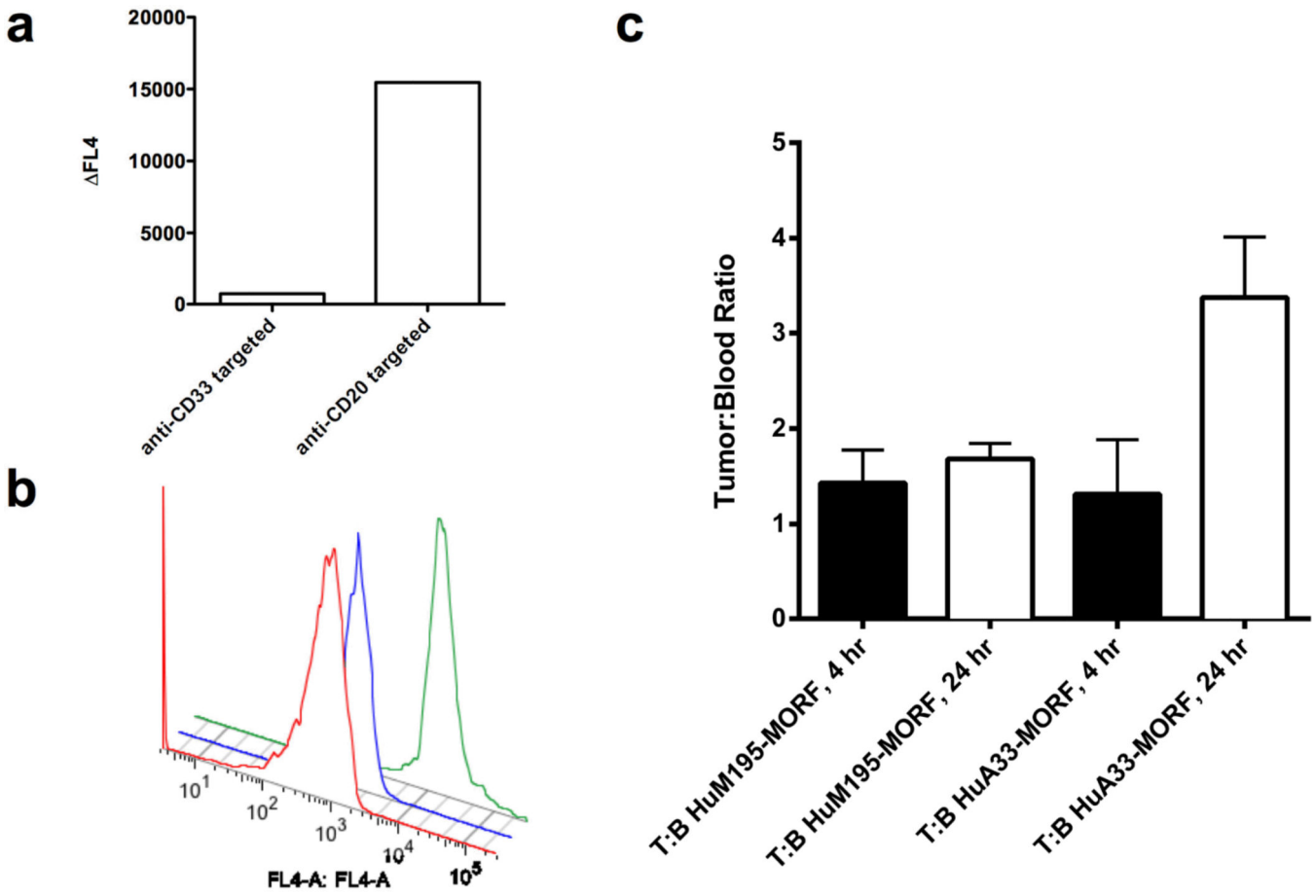


**Figure 4. SWNT-cMORF can selectively self-assemble onto pretargeted tumours in-vivo**

**(a)** Flow cytometric analysis of CD20 positive, CD33 negative Daudi-GFP cells harvested from mice treated with either isotype control anti-CD33-MORF, or tumour specific anti-CD20-MORF. Data show the shift in median fluorescence from untreated Daudi-GFP cells (representative mice are shown). The SWNT-cMORF bound selectively to the tumour cells in mice pre-targeted with specific antibody as evidenced by the 20-fold increase over the control. (b) Representative flow cytometric histograms of data in panel (a) shows untreated cells (red), isotype mAb-MORF (anti-CD33-MORF) treated cells (blue), and specific mAb-MORF (anti-CD20-MORF) treated cells (green). (c) Tumour to blood ratios (T:B) for LS174T tumoured mice pretargeted with either specific anti-A33-MORF or isotype control anti-CD33-MORF followed by injection of SWNT-cMORF-$^{111}$In(DOTA). Signal measurements in %ID per gram were measured at 4 or 24 hours post injection of injection of SWNT-cMORF-$^{111}$In(DOTA). There was a significant increase ($p<0.05$) in tumour accumulation of SWNT-cMORF-$^{111}$In(DOTA) at the tumour site only when pre-targeted with specific antibody as compared to isotype control.

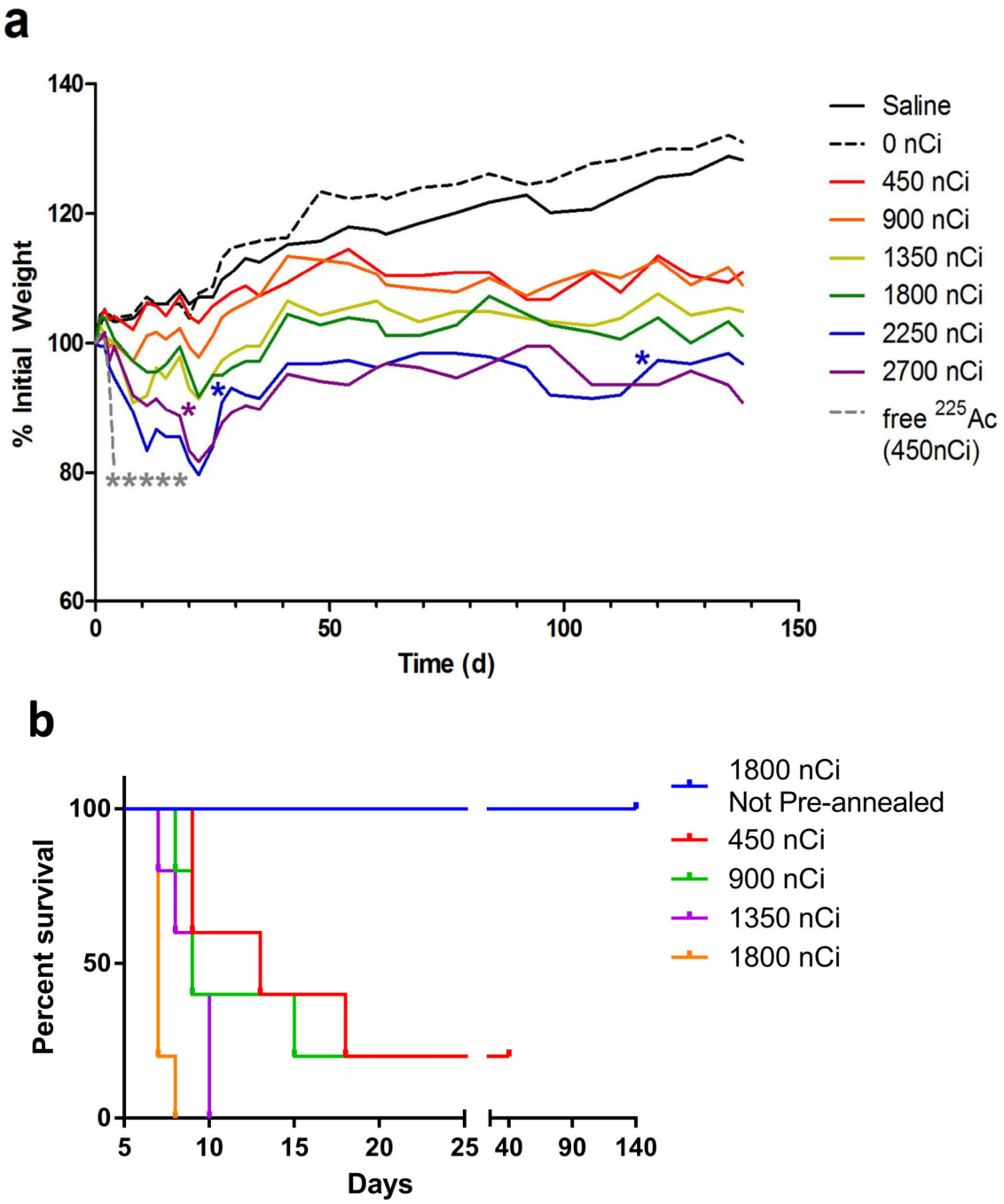


**Figure 5. SWNT-cMORF-($^{225}$Ac)DOTA mitigates radioisotope toxicity and can be used as an effective agent in multistep therapy of disseminated lymphoma**

**(a)** Whole animal weights of tumour-free mice treated with varying dose levels of $^{225}$Ac labeled SWNT-cMORF-DOTA. An additional group of mice received 450 nCi of free $^{225}$Ac as a control. Data reflect average weights, n=5 for all groups. Each animal death is noted by a single asterisk. Toxicity study was halted at 140 days. Median survival was greater than 20 weeks in all groups **(b)** Kaplan-Meier plot of pre-annealed “single-step” treatment mouse

survival with comparison to not annealed **(a)** 1800 nCi group from Fig 5a.. Toxicity study was halted at 40 days. Median survival was less than 2 weeks in all groups.

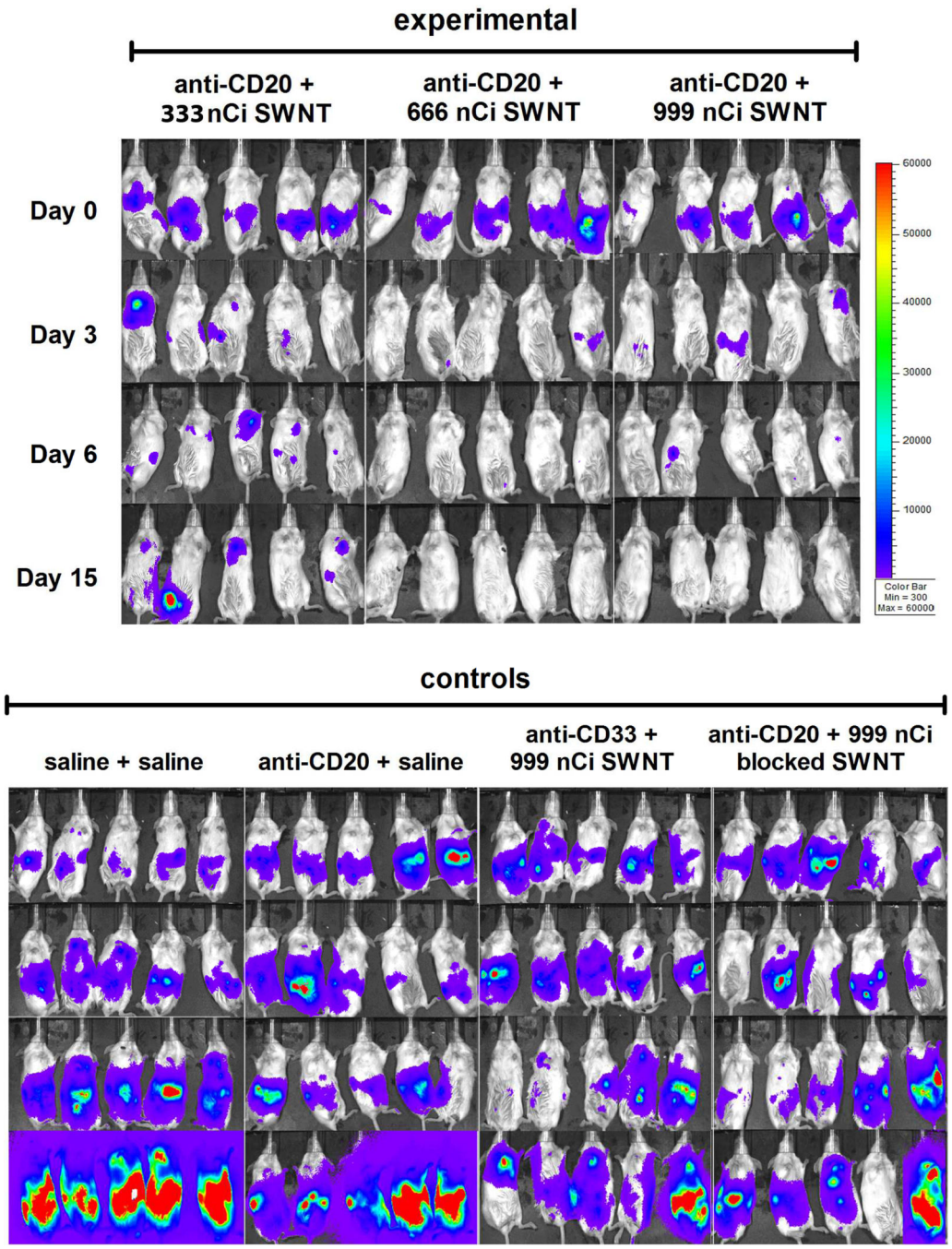


**Figure 6. SWNT-cMORF-($^{225}$Ac)DOTA can be used as an effective agent in multistep therapy of disseminated lymphoma**

Mice previously implanted with luciferase-transfected Daudi lymphoma cells were injected with 5mg/ml luciferin and imaged after a 5 minute delay. The parameters are equivalent for all images, but as a trade-off, this leads to saturation that disallows quantification. Mice were treated with multistep therapy as previously noted and imaged at days 0, 3, 6, and 15 post treatment. Growth, Rituximab therapy, isotype high-dose radiation, and blocked 2-step controls are provided. For further controls see also Figure S8.

**Table 1**

Control and experimental groups for SWNT-cMORF-225Ac(DOTA) therapy of Daudi lymphoma

| **Group** | **Injection 1, 0h(200uL)** | **Injection 2, 24h (200 uL)** |
|---|---|---|
| 1 Untreated Control | Saline | Saline |
| 2 Anti-CD20 alone control | 1.5ug anti-CD20-MORF | Saline |
| 3 Unlabeled SWNT Control | Saline | SWCNT-cMORF-DOTA (**0** nCi $^{225}$Ac) (3.57ug) |
| 4 Isotype control | 1.5ug anti-CD33-MORF | SWCNT-cMORF-DOTA (**333**nCi $^{225}$Ac) (1.19ug) |
| 5 Isotype control | 1.5ug anti-CD33-MORF | SWCNT-cMORF-DOTA (**666**nCi $^{225}$Ac) (2.38ug) |
| 6 Isotype control | 1.5ug anti-CD33-MORF | SWCNT-cMORF-DOTA (**999**nCi $^{225}$Ac) (3.57ug) |
| 7 Treatment group | 1.5ug Anti-CD20-MORF | SWCNT-cMORF-DOTA (**333**nCi $^{225}$Ac) (1.19ug) |
| 8 Treatment group | 1.5ug Anti-CD20-MORF | SWCNT-cMORF-DOTA (**666**nCi $^{225}$Ac) (2.38ug) |
| 9 Treatment group | 1.5ug Anti-CD20-MORF | SWCNT-cMORF-DOTA (**999**nCi $^{225}$Ac) (3.57ug) |
| 10 Blocked treatment group “Dual Control” | 1.5ug Anti-CD20-MORF | MORF Blocked SWCNT-cMORF-DOTA (**999**nCi $^{225}$Ac) (3.57ug) |